ФИЗИКА

УДК 539.3;621.382 DOI: https://doi.org/10.54341/20778708_2024_1_58_29
EDN: SWGRMA

ОПТИМИЗАЦИЯ ПАРАМЕТРОВ ДВУЛУЧЕВОГО ЛАЗЕРНОГО РАСКАЛЫВАНИЯ СТЕКЛОИЗДЕЛИЙ ТРУБЧАТОЙ ФОРМЫ

Ю.В. Никитюк[1], В.А. Емельянов[2], Е.Б. Шершнев[1], Ц. Ма[3], Л. Ван[3], И.Ю. Аушев[4]

[1]*Гомельский государственный университет имени Франциска Скорины*
[2]*ОАО «Интеграл», Минск*
[3]*Нанкинский университет науки и технологий*
[4]*Университет гражданской защиты, Минск*

OPTIMIZATION OF PARAMETERS FOR DOUBLE-BEAM LASER CLEAVING OF TUBULAR-SHAPED GLASS PRODUCTS

Yu.V. Nikityuk[1], V.A. Emelyanov[2], E.B. Shershnev[1], J. Ma[3], L. Wang[3], I.Yu. Aushev[4]

[1]*Francisk Skorina Gomel State University*
[2]*JSC "INTEGRAL", Minsk*
[3]*Nanjing University of Science and Technology*
[4]*University of Civil Protection of the Ministry for Emergency Situations of the Republic of Belarus, Minsk*

Аннотация. При помощи конечно-элементных расчетов получены регрессионные и нейросетевые модели процесса двулучевого лазерного раскалывания стеклоизделий трубчатой формы. С использованием центрального композиционного плана проведен соответствующий численный эксперимент, в котором скорость вращения стеклянной трубки, геометрические параметры эллиптического лазерного пучка с длиной волны 10,6 мкм и мощности лазерных пучков с длинами волн 10,6 мкм и 1,06 мкм использовались в качестве варьируемых факторов. При этом значения максимальных температур и максимальных термоупругих напряжений растяжения в зоне двулучевой обработки стеклянных трубок определялись в качестве откликов в рамках конечно-элементного моделирования с использованием языка программирования APDL. При помощи библиотеки для машинного обучения TensorFlow выявлены эффективные архитектуры искусственных нейронных сетей для определения максимальных температур и максимальных термоупругих напряжений в зоне лазерной обработки. Проведено сравнение нейросетевых и регрессионных моделей. С использованием генетического алгоритма MOGA проведена многокритериальная оптимизация параметров двулучевого лазерного раскалывания стеклоизделий трубчатой формы.

Ключевые слова: *лазерная резка*, *трещина*, *ИНН*, *MOGA*, *ANSYS*.

Для цитирования: *Оптимизация параметров двулучевого лазерного раскалывания стеклоизделий трубчатой формы* / Ю.В. Никитюк, В.А. Емельянов, Е.Б. Шершнев, Ц. Ма, Л. Ван, И.Ю. Аушев // Проблемы физики, математики и техники. – 2024. – № 1 (58). – С. 29–35. – DOI: https://doi.org/10.54341/20778708_2024_1_58_29. – EDN: SWGRMA

Abstract. This study used finite-element calculations to develop regression and neural network models for the double-beam laser cleaving process of tubular-shaped glass products. A numerical experiment was performed using the central composite design, where the rotation speed of the glass tube, the geometric parameters of an elliptical laser beam with a wavelength of 10.6 μm, and the powers of laser beams with wavelengths of 10.6 μm and 1.06 μm were used as variable factors. The maximum temperatures and maximum thermoelastic tensile stresses in the zone of double-beam processing of glass tubes were determined as responses using finite element modelling with APDL (Ansys Parametric Design Language). The effective architectures for artificial neural networks have been established with TensorFlow in order to determine the maximum temperatures and thermoelastic stresses in the laser-treated area. The comparative analysis of neural network and regression models was carried out. A multi-criteria optimization of the parameters of double-beam laser cleaving of tubular-shaped glass products was performed using MOGA (multi-objective genetic algorithm).

Keywords: *laser cutting*, *crack*, *ANN*, *MOGA*, *ANSYS*.

For citation: *Optimization of parameters for double-beam laser cleaving of tubular-shaped glass products* / Yu.V. Nikityuk, V.A. Emelyanov, E.B. Shershnev, J. Ma, L. Wang, I.Yu. Aushev // Problems of Physics, Mathematics and Technics. – 2024. – № 1 (58). – P. 29–35. – DOI: https://doi.org/10.54341/20778708_2024_1_58_29 (in Russian). – EDN: SWGRMA

Introduction

Silicate glasses possess qualities that make them very suitable for industrial applications, with cutting being the main technique involved in the creation of glass products. Laser cleaving technology offers several notable advantages when compared to conventional cutting methods. The advancement of laser cleaving technology occurred in the latter part of the twentieth century. However, even now, the investigation of laser cleaving methods for separating different brittle non-metallic materials remains significant [1]–[4].

Laser cleaving of tubular-shaped glass products is a highly practical and significant technology.

The initial findings about the cleaving method for laser cutting of glass tubes are outlined in [2]. The exceptional effectiveness of double-beam techniques in cutting plane-parallel samples using laser cleaving methods served as the foundation for developing double-beam variations of laser cleaving for tubular-shaped glass products [5]–[8].

Metamodels are a reasonable choice when optimizing the parameters of laser cleaving for brittle nonmetallic materials. Metamodeling enables the identification of laser processing output parameters by employing regression and neural network models, eliminating the need for extensive calculations. Simultaneously, using genetic algorithms in metamodeling allows for the determination of the optimal values for laser cleaving parameters [9]–[15].

This study investigates the process of double-beam laser cleaving of tubular-shaped glass products using finite-element, regression and neural network models, and determines the effective parameters of laser-induced crack formation via MOGA (multi-objective genetic algorithm).

1 Determination of optimal parameters for double-beam laser cleaving of tubular-shaped glass products

Figure 1.1 depicts the schematic of a double-beam laser cleaving process used for tubular-shaped glass products. Position 1 relates to the CO_2 laser, position 2 corresponds to the refrigerant supply nozzle, and position 3 refers to the YAG laser.

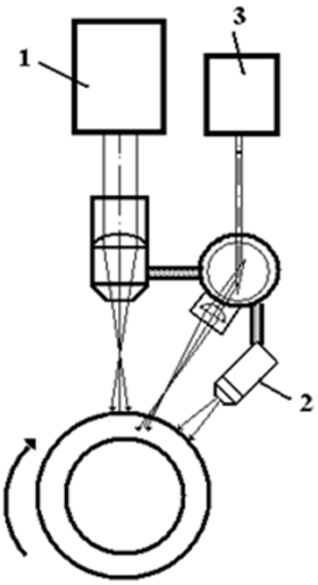

Figure 1.1 – Schematic of double-beam laser cleaving of tubular-shaped glass products

During the modelling process, it was taken into account that the tubular-shaped glass product is heated by laser radiation over several revolutions, while the tube surface is concurrently cooled by an air-water mixture at a certain distance from the laser heating zones.

The temperatures and thermoelastic stresses generated in tubular-shaped glass products during double-beam laser cleaving were determined using APDL. The characteristics of silicate glass provided in reference [2] were used in the modelling process. The calculations were conducted for a tube with an outer radius of 5 mm, an inner radius of 4 mm, and a length of 10 mm. The model comprised 4352 Solid 5 elements (see Figure 1.2).

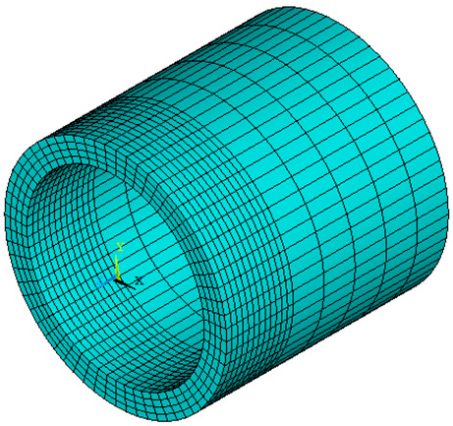

Figure 1.2 – Finite element model

The subsequent parameters were employed for the purpose of modelling: the tube's rotation speed relative to the laser beams was set at 40 revolutions per minute; the laser beam with a radiation wavelength of $\lambda = 10.6$ μm had a radiation power of $P = 5$ W; the major semi-axis of the laser beam was $A = 3 \cdot 10^{-3}$ m, and the minor semi-axis was $B = 1 \cdot 10^{-3}$ m; the laser beam with a radiation wavelength of $\lambda = 1.06$ μm had a radiation power of $P_0 = 50$ W; the radiation spot radius was $R = 0.5 \cdot 10^{-3}$ m.

The calculated values of the temperature fields and the thermoelastic stress fields created in a tubular-shaped glass product during double-beam laser cleaving are depicted in Figures 1.3–1.4.

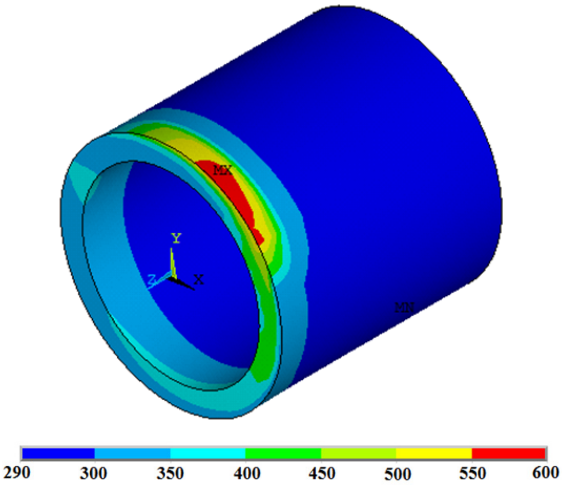

Figure 1.3 – Temperature distribution throughout the sample's volume, °K

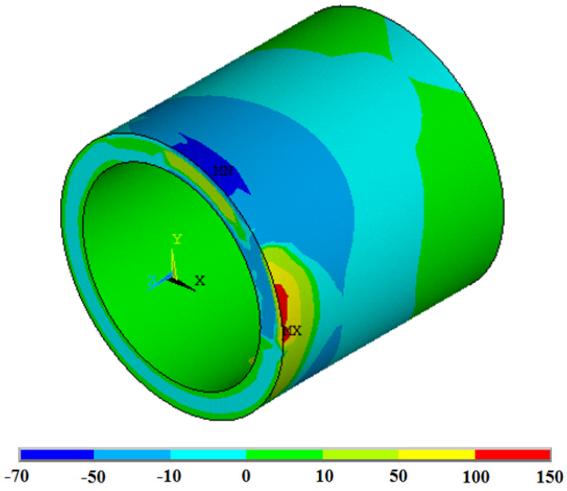

Figure 1.4 – Distribution of stresses σ_{zz} throughout the sample's volume, MPa

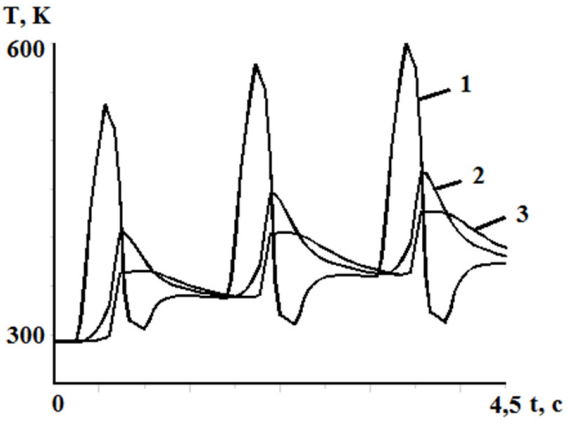

Figure 1.5 – Computed relationships between temperature *T* and processing time at specific points along the tube

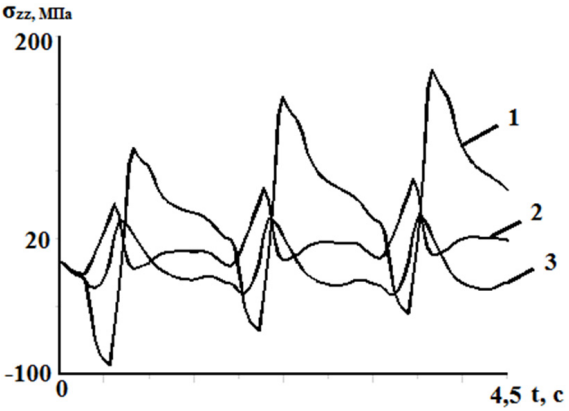

Figure 1.6 – Computed relationships between stresses σ_{zz} and processing time at specific points along the tube

Figures 1.5, 1.6 display the calculated relationships between temperatures and thermoelastic stresses in the axial direction of the tube over time. These relationships are shown at specific points on the cutting plane (1 represents the outer surface of the tube; 2 stands for the middle of the tube wall; 3 indicates the inner surface of the tube). These calculations were made during the process of double-beam cleaving.

The maximum temperatures calculated for the finite element modelling parameters did not surpass the glass transition temperature of the processed material (795 K for C52 glass), which is a prerequisite for the occurrence of laser-induced cracks (see Figures 1.3 and 5) [2].

When a glass tube is subjected to multiple laser heating while rotating around its axis, the temperature at specific points on its surface in the cutting plane experiences periodic sharp increases and decreases due to the refrigerant's impact. Simultaneously, there is a slight increase in the maximum temperatures of the glass and the maximum thermoelastic stresses exerted in the axial direction of the tube with each revolution in relation to the laser radiation sources (see Figures 1.5, 1.6). Furthermore, additional exposure to YAG-laser radiation results in elevated tensile and compressive stresses, hence enhancing the stability of laser-induced crack formation.

2 The numerical experiment

The numerical experiment was carried out using 27 combinations of the face-centered version of the central composite design generated in the DesignXplorer module for five factors (P1-P5): P1 was the rotation speed of the tube ω; P2 was the laser power with radiation wavelength λ = 10.6 μm P; P3 was the major semi-axis of the laser beam A with radiation wavelength λ = 10.6 μm; P4 was the minor semi-axis of the beam B with radiation wavelength λ = 10.6 μm; P5 was the laser power with radiation wavelength λ = 10.6 μm P_0. The following responses were determined: maximum temperature T and maximum tensile stresses σ_{zz} in the treatment zone (see Table 2.1).

The response functions relating the output parameters (T, σ_{zz}) to the factors (ω, P, A, B, P_0) take the following form:

$$Y_T = 6.69 - 6.67\cdot10^{-3}\omega + 0.155P - 751B +$$
$$+1.68\cdot10^{5}B^2 - 3.68\cdot10^{-4}\omega P + 1.09\omega B - 6.72PA -$$
$$- 31.2PB - 2.29\cdot10^{-4}PB_0 + 1.27\cdot10^{4}AB +$$
$$+ 0.106AP_0 + 2.09BP_0,$$
$$T = e^{Y_T} - 1,$$
$$Y_\sigma = -6.74\cdot10^{8} - 5.03\cdot10^{8}\omega P + 2.23\cdot10^{9}\omega A +$$
$$+1.85\cdot10^{5}\omega P_0 - 9.4\cdot10^{10}PB - 5.06\cdot10^{5}PP_0 +$$
$$+3.44\cdot10^{9}BP_0,$$
$$\sigma_{zz} = (1.17Y_\sigma + 1)^{\frac{1}{1.17}} - 1.$$

Figure 2.1 depicts the assessment of how the input parameters affect the output parameters. Both responses during double-beam laser cleaving of

tubular-shaped glass products are significantly influenced by tube rotation speed ω and laser power with radiation wavelength λ = 10.6 μm. At the same time, the values of the maximum tensile stresses σ_{zz} are substantially affected by the laser power with radiation wavelength λ = 10.6 μm.

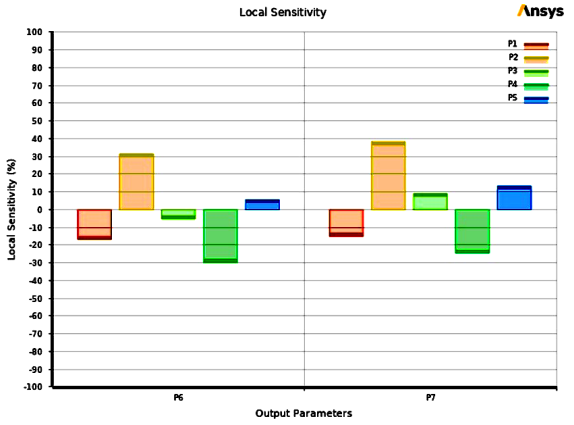

Figure 2.1 – Response sensitivity diagram $P1$ – ω, $P2$ – P, $P3$ – A, $P4$ –B, $P5$ – P_0, $P6$ – T, $P7$ – σ_{zz}

Figures 2.2, 2.3 show the dependences of maximum temperatures T and maximum tensile stresses σ_{zz} in the treatment zone on the processing parameters.

The construction of artificial neural networks containing two hidden layers (see Figure 2.4) was performed using TensorFlow in accordance with the algorithm outlined in [16].

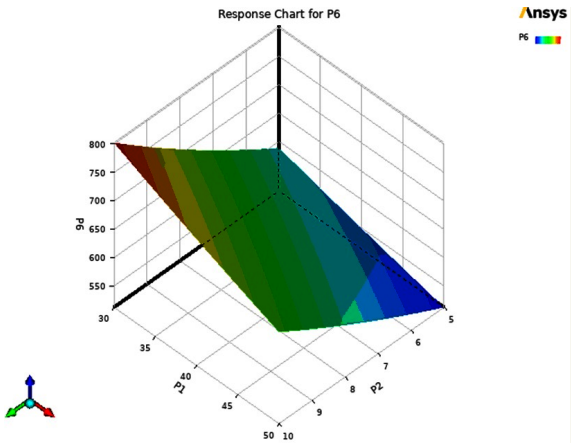

Figure 2.2 – Dependence of maximum temperature T, K on processing parameters $P1$ = ω ,$P2$ = P

The Adam optimizer, ReLU activation function, and MSE loss function were applied in the process of constructing the artificial neural network. The neural network underwent training for a total of 500 epochs. Consequently, 16 artificial neural networks were created with the number of neurons in two hidden layers ranging from 5 to 20, with an interval of 5.

Table 2.1 – Experimental design and calculation results

№	$P1$ ω, rev / min	$P2$ P, W	$P3$ A, m	$P4$ B, m	$P5$ P_0, W	$P6$ T,°K	$P7$ σ_{zz}, MPa
1	40	7.5	0.003	0.0015	65	632	82.1
2	30	7.5	0.003	0.0015	65	690	85.8
3	50	7.5	0.003	0.0015	65	591	76.2
4	40	5	0.003	0.0015	65	551	66.8
5	40	10	0.003	0.0015	65	731	97.5
6	40	7.5	0.002	0.0015	65	651	72.7
7	40	7.5	0.004	0.0015	65	617	84.7
8	40	7.5	0.003	0.001	65	762	93.0
9	40	7.5	0.003	0.002	65	575	71.7
10	40	7.5	0.003	0.0015	50	622	73.8
11	40	7.5	0.003	0.0015	80	652	90.4
12	30	5	0.002	0.001	80	714	76.5
13	50	5	0.002	0.001	50	585	54.7
14	30	10	0.002	0.001	50	1055	124.1
15	50	10	0.002	0.001	80	866	99.3
16	30	5	0.004	0.001	50	632	70.1
17	50	5	0.004	0.001	80	588	80.0
18	30	10	0.004	0.001	80	959	129.2
19	50	10	0.004	0.001	50	785	99.8
20	30	5	0.002	0.002	50	534	48.7
21	50	5	0.002	0.002	80	512	57.8
22	30	10	0.002	0.002	80	737	92.3
23	50	10	0.002	0.002	50	598	60.5
24	30	5	0.004	0.002	80	587	71.2
25	50	5	0.004	0.002	50	462	49.2
26	30	10	0.004	0.002	50	661	89.8
27	50	10	0.004	0.002	80	603	87.5

Table 2.2 – Test dataset

№	*P*1 ω, rev / min	*P*2 *P*, W	*P*3 *A*, m	*P*4 *B*, m	*P*5 P_0, W	*P*6 *T*,°K	*P*7 σ_{zz}, MPa
1	38	8.4	0.003	0.002	54	592	70.8
2	40	9.7	0.002	0.001	68	927	105.8
3	35	7.8	0.003	0.002	51	584	67.4
4	31	7.4	0.002	0.002	72	639	70.1
5	36	9.2	0.004	0.001	60	843	109.4
6	44	8.1	0.003	0.001	68	772	96.7
7	36	8.3	0.004	0.001	61	793	102.6
8	34	6.5	0.004	0.001	77	719	97.2
9	50	5.1	0.003	0.002	72	499	60.5
10	35	7.6	0.003	0.001	60	801	93.4

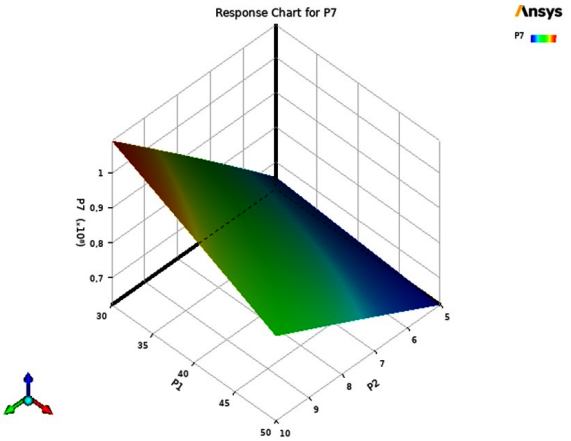

Figure 2.3 – Dependence of maximum stresses σ_{zz}, MPa on processing parameters *P*1 = ω, *P*2 = *P*

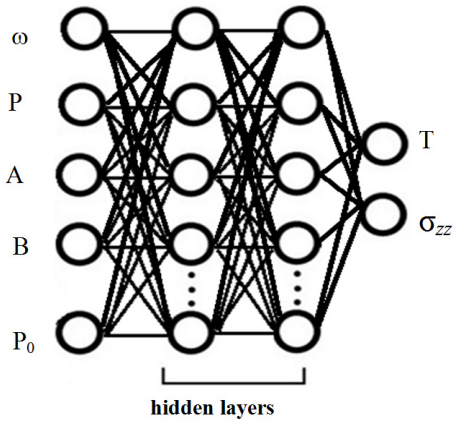

Figure 2.4 – Artificial neural network architecture

The dataset presented in Table 2.2 was used to perform tests on regression and neural network models.

The resulting models were evaluated using mean absolute error (MAE), root mean square error (RMSE), mean absolute percentage error (MAPE), and determination coefficient R^2.

Figures 1.11, 1.12 show heat maps illustrating the distribution of validation errors in determining the maximal values of temperature and tensile stresses during double-beam laser cleaving of tubular-shaped glass products. The number of neurons in the first and second hidden layers of the artificial neural network are shown by the vertical and horizontal axes, respectively. The intensity of color coding represents the extent of error: the error increases from light to dark.

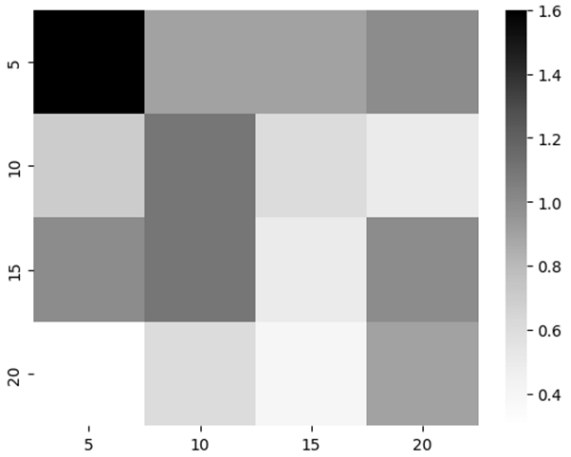

Figure 2.5 – Heat map of MAPE error distribution when determining *T*

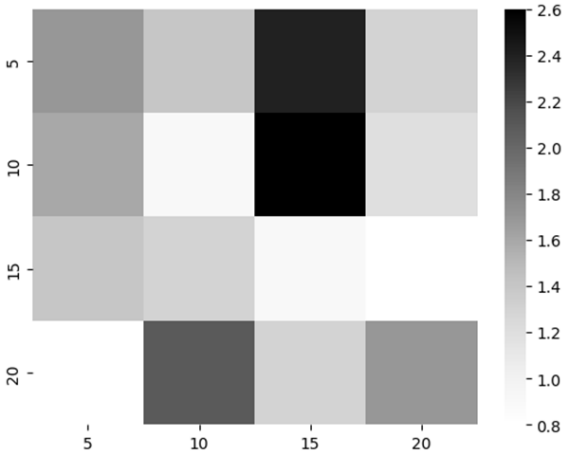

Figure 2.6 – Heat map of MAPE error distribution when determining σ_{zz}

The artificial neural network with the architecture [5-20-5-2] demonstrated the most favorable results when determining the values of maximum

temperatures T and the maximum tensile stresses σ_{zz} in the treatment zone.

Table 2.3 displays the estimation outcomes of both the regression and neural network models.

Table 2.3 – Evaluation results of regression and neural network models

Criterion	Regression model		Neural network model	
	T	σ_{zz}	T	σ_{zz}
RMSE	6.4 K	2.78 MPa	2.4 K	0.80 MPa
MAE	5.9 K	2.36 MPa	2.0 K	0.66 MPa
MAPE	0.8 %	2.7 %	0.3 %	0.8%
R^2	0.9975	0.9739	0.9998	0.9993

The evaluation findings of the generated regression and neural network models demonstrate a required consistency with the outcomes obtained from finite element computations. Neural network models exhibit higher efficiency when it comes to predicting the parameters of double-beam laser cleaving of tubular-shaped glass products.

The MOGA algorithm of the DesignXplorer module was used to perform multicriteria optimization of parameters for double-beam laser cleaving of tubular-shaped glass products. The optimization procedures were conducted in accordance with the algorithm outlined in [10].

The following optimization criteria were chosen: $\omega \rightarrow \max$, $\sigma_{zz} \rightarrow \max$, $T \leq 795$ K. The optimization results are provided in Table 2.4. Parameter values derived using the finite element modeling are presented in brackets. The application of the MOGA algorithm provided the maximum relative error of less than 3% when determining the responses.

Table 2.4 – Optimization results

№	1
*P*1 ω, rev / min	49.8
*P*2 *P*, W	9.9
*P*3 *A*, m	0.004
*P*4 *B*,	0.001
*P*5 P_0, W	79
*P*6 *T*, °K	794 (778)
*P*7 σ_{zz}, MPa	111,7 (115.1)

Conclusion

This study presents the construction of regression and neural network models of double-beam laser cleaving of tubular-shaped glass products and determines the optimal neural network architecture, the accuracy of which was found to be superior to that of the corresponding regression models. The application of the MOGA algorithm in multicriteria optimization has led to the identification of modes for double-beam laser cleaving, which ensure efficient generation of laser-induced cracks in glass tubes.

REFERENCES

1. *Lumley*, *R.M*. Controlled separation of brittle materials using a laser / R.M. Lumley // Am. Ceram. Soc. Bull. – 1969. – Vol. 48. – P. 850–854.

2. *Machulka*, *G.A*. Laser processing of glass / G.A. Machulka. – Moscow: Sov. radio, 1979. – 136 p. (In Russian).

3. *Nisar*, *S*. Laser glass cutting techniques. – A review / S. Nisar // Journal of laser applications. – 2013. – Vol. 25, № 4. – P. 042010-1–11.

4. *Kondratenko*, *V.S*. Precision Cutting of Glass and Other Brittle Materials by Laser-Controlled Thermo-Splitting (Review) / V.S. Kondratenko, S.A. Kudzh // Glass Ceram. 74. – 2017. – P. 75–81. – DOI: https://doi.org/10.1007/s10717-017-9932-1.

5. *Two-beam laser thermal cleavage of brittle nonmetallic materials* / S.V. Shalupaev, E.B. Shershnev, Yu.V. Nikityuk, A.A. Sereda // Journal of Optical Technology. – 2006. – Vol. 73, № 5. – P. 356–359. – DOI: 10.1364/JOT.73.000356.

6. *Dual laser beam revising the separation path technology of laser induced thermal-crack propagation for asymmetric linear cutting glass* / C. Zhao, H. Zhang, L. Yang [et al.] // International Journal of Machine Tools and Manufacture. – 2016. – Vol. 106. – P. 43–55. – DOI: 10.1016/j.ijmachtools.2016.04.005.

7. *Nikityuk*, *Yu.V*. Physical regularities of laser thermal cleaving of silicate glasses and alumina ceramics: specialty 01.04.21 “Laser physics”: PhD thesis extended abstract / Nikityuk Yuri Valerievich. – Minsk, 2009. – 24 p. (In Russian).

8. *Shalupaev*, *S.V*. Laser thermal cleaving of tubular-shaped glass products / S.V. Shalupaev, Yu.V. Nikityuk // Problems of Physics, Mathematics and Technology. – 2010. – № 3 (4). – P. 35–40 (In Russian).

9. *Nikityuk*, *Yu.V*. Optimization of parameters for laser cleaving of quartz glass / Yu.V. Nikityuk, A.N. Serdyukov, I.Yu. Aushev // Problems of Physics, Mathematics and Technics. – 2021. – № 4 (49). – P. 21–28. – DOI: 10.54341/20778708_2021_4_49_21. (In Russian).

10. *Nikityuk*, *Yu.V*. Optimization of two-beam laser cleavage of silicate glass / Yu.V. Nikityuk, A.N. Serdyukov, I.Yu. Aushev // Journal of Optical Technology. – 2022. – Vol. 89, № 2. – P. 121–125. – DOI: 10.1364/JOT.89.000121.

11. *Nikityuk*, *Yu.V*. Optimization of laser splitting parameters of silicate glasses with elliptical beams in the plane of parallel surface / Yu.V. Nikityuk, A.N. Serdyukov, I.Yu. Aushev // Vestnik of the Sukhoi State Technical University of Gomel. – 2023. – № 3. – P. 17–27.

12. *Nikityuk*, *Yu.V*. Optimization of laser cleaving of silicate glasses with elliptical beams using fracture mechanics parameters / Yu.V. Nikityuk, I.Yu. Aushev // Problems of Physics, Mathematics and Technics. – 2023. – № 4 (57). – P. 36–41.

13. *Nikityuk*, *Y*. Determination of the Parameters of Controlled Laser Thermal Cleavage of Crystalline Silicon Using Regression and Neural Network Models / Y. Nikitjuk, A. Serdyukov // Crystallography Reports. – 2023. – Vol. 68, № 7. – P. 195–200.

14. *Parametric optimization of silicate-glass-based asymmetric two-beam laser splitting* / Yu. Nikityuk, A. Sereda, A. Serdyukov, S. Shalupaev, I. Aushev // Journal of Optical Technology. 2023. – Vol. 90, iss. 6. – P. 296–301. – DOI: https://doi.org/10.1364/JOT.90.000296.

15. *Nikityuk*, *Yu.V*. Optimization of laser cleaving of silicate glasses by elliptical beams under additional influence of hot air flow / Yu.V. Nikityuk, A.N. Serdyukov, I.Yu. Aushev // Proceedings of F. Skorina Gomel State University. – 2023. – № 6 (141). – P. 110–116. (In Russian).

16. *Nikityuk*, *Yu.V*. Determination of the parameters of two-beam laser splitting of silicate glasses using regression and neural network models / Yu.V. Nikityuk, A.N. Serdyukov, I.Yu. Aushev // Journal of the Belarusian State University. Physics. – 2022. – № 1. – P. 35–43. – DOI: https://doi.org/10.33581/2520-2243-2022-1-35-43.

The article was submitted 18.12.2023.

Информация об авторах

Никитюк Юрий Валерьевич – к.ф.-м.н., доцент
Емельянов Виктор Андреевич – чл.-корр. НАН Беларуси, д.т.н., профессор
Шершнев Евгений Борисович – к.т.н., доцент
Ма Цзюнь – профессор
Ван Лей – доцент
Аушев Игорь Юрьевич – к.т.н., доцент